ACTA ASTRONOMICA
Vol. **57** (2007) pp. 249–266

The Optical Gravitational Lensing Experiment. Variable Stars in the Field of Open Cluster NGC 6755*

A. Ciechanowska[1], G. Pietrzyński[1,2], Z. Kołaczkowski[2,3], Ł. Wyrzykowski[1,4], O. Szewczyk[1,2], M. Kubiak[1], A. Udalski[1] and M. K. Szymański[1]

[1] Warsaw University Observatory, Al. Ujazdowskie 4, 00-478 Warszawa, Poland
e-mail:(aciechan,pietrzyn,wyrzykow,mk,udalski,msz)@astrouw.edu.pl
[2] Universidad de Concepción, Departamento de Fisica, Astronomy Group, Casilla 160-C, Concepción, Chile
e-mail:(zibi,szewczyk)@astro-udec.cl
[3] Astronomical Institute, University of Wroclaw ul. Kopernika 11, 51-622 Wroclaw, Poland
[4] Institute of Astronomy, University of Cambridge, Madingley Road, Cambridge CB3 0HA, United Kingdom
e-mail: wyrzykow@ast.cam.ac.uk

Received September 12, 2007

ABSTRACT

We present the results from a search for variable stars in the field of a young open cluster NGC 6755. Altogether seventy one variable stars have been discovered. Thirty one of them are eclipsing systems. This group contains ten EA, four EB and seventeen EW-type systems. Photometric variability of four late type stars is most probably caused by their chromospherical activity. Another seven detected variable stars have light curves typical for pulsating stars from the main instability strip. Four of them we tentatively classified as γ Dor, one as δ Sct and two as Population II Cepheid variable stars, respectively. Star designated as V40 can be either another population II Cepheid or an ellipsoidal binary system. The remaining twenty eight variable stars found in the field of this open cluster are most probably highly obscured background red giants (OSARG, irregular). For all detected variable stars we provide their light curves, preliminary classification, discussion on the possible cluster membership, equatorial coordinates, finding charts and periods when possible.

Key words: *binaries: eclipsing – Stars: oscillations – open clusters and associations: individual: NGC 6755*

*Based on observations obtained with the 1.3-m Warsaw telescope at the Las Campanas Observatory of the Carnegie Institution of Washington.

1. Introduction

Star clusters are perfect laboratories for testing stellar evolution, pulsational and dynamical theories, because all stars in a given cluster can be assumed to have similar age, distance, and chemical composition. Variable stars provide an additional and independent information on the distance, age, mass and diameters of individual stars in the cluster. Unfortunately, the number of such objects known in open clusters is still very small. Therefore we have started on a long term project which aims at systematic survey for variable stars in about a dozen of relatively young open clusters. We already published the results for NGC 654 (Pietrzyński 1996a), IC 4996 (Pietrzyński 1996b), NGC 663 (Pietrzyński 1997), NGC 5381 (Pietrzyński *et al.* 1997), NGC 5999 (Pietrzyński *et al.* 1998), NGC 659 (Pietrzyński *et al.* 2001), NGC 581 (Wyrzykowski *et al.* 2002) and NGC 6259 (Ciechanowska *et al.* 2006). In this contribution, variable stars detected in the field of another young open cluster, NGC 6755 are presented.

Basic information on this poorly studied cluster, taken from Kjeldsen and Frandsen (1991), is given in Table 1. As far as we know this cluster has not yet been surveyed for variable stars.

Table 1

Basic data about NGC 6755

α (2000)	$19^{\mathrm{h}}07^{\mathrm{m}}49^{\mathrm{s}}$
δ (2000)	$+04^\circ16'00''$
d [pc]	2150
$V-M_V$ [mag]	14.10
$(m-M)_0$ [mag]	11.65
$\log t$ [log (years)]	8.40
$E(B-V)$ [mag]	0.77

2. Observations and Data Reductions

The presented data were collected from July 1997 to September 1999 during twenty seven nights in the course of the OGLE project (Udalski, Kubiak, Szymański 1997) at the time, when the weather conditions were too poor to observe the very dense main OGLE fields. All observations were made with 1.3-m Warsaw telescope located at the Las Campanas Observatory, Chile which is operated by the Carnegie Institution of Washington. The telescope was equipped with a 2048×2048 pixels CCD camera with the field of view of $14\overset{'}{.}2\times14\overset{'}{.}2$ and the scale of $0\overset{''}{.}417$/pixel. Instrument and data acquisition system are described in details in Udalski *et al.* (1998). Most observations were taken through the Cousins I-band filter, but in order to obtain information about the $V-I$ color a single image through the Johnson *V*-band filter was also made. Bias subtraction and flatfielding were performed with the IRAF[†] package. Aperture and profile photometries were obtained with DAOPHOT and ALLSTAR programs. Due to the fact that the PSF changes across the chip it was not possible to obtain good photometry assuming a constant PSF. Therefore all frames were divided into 16 overlapping subframes. The size of each subframe was 512×512 pixels with 100-pixels margins. Each of them was reduced independently assuming a constant PSF model.

3. Search for Variable Stars

Because of the fact that the *V*-band data were obtained on just one epoch, for searching for variable stars only the *I*-band photometry was used. In order to create the database, we selected the image taken at the best seeing conditions. Then the master list with positions of all stars from this template image was constructed. The resulting database contains 31 427 stars, where the faintest objects have *I*-band magnitudes of about 20 mag. Next, we rejected all stars, which have less than about 30% measurements (*i.e.*, we analyzed only those with at least 57 photometric data points). All the remaining objects were subject of search for variable stars performed in the same way as in Ciechanowska *et al.* (2006). Shortly, for all of these stars we computed the dispersion of brightness (σ) and the mean error returned by DAOPHOT ($\sigma_{\rm DAO}$). Based on the analysis of all light curves in one of the subframes we found that all candidates for variable stars had the ratio $\sigma/\sigma_{\rm DAO}$ greater than 2.3, so in the remaining subframes only such stars were searched for variability using the AoV algorithm (Schwarzenberg-Czerny, 1986) and FNPEAKS software (Kolaczkowski, private communication). Obtained periodograms were examined visually in order to derive periods, to settle type of star variability and to reject cases, when big value of $\sigma/\sigma_{\rm DAO}$ ratio was accidental (*e.g.*, for stars located close to the edge of the frame, close to a bright and saturated star, etc.). In order to detect stars showing photometric variability of irregular nature apart from analysis of their periodograms the light curves of all selected candidates were also visually inspected. The identified variable stars are presented and briefly discussed in Section 4.

4. Transformations

For the transformation purpose, we used a pair of images in *V* and *I*-bands, obtained at the night, when measurements of photometric standards were routinely

---

[†]IRAF is distributed by National Optical Observatories, which is operated by Association of Universities for Research in Astronomy, Inc., under cooperative agreement with National Science Foundation.

performed in the course of the OGLE II project (HJD = 2451078.53) Those frames were reduced in an exactly the same way as described in Section 2.

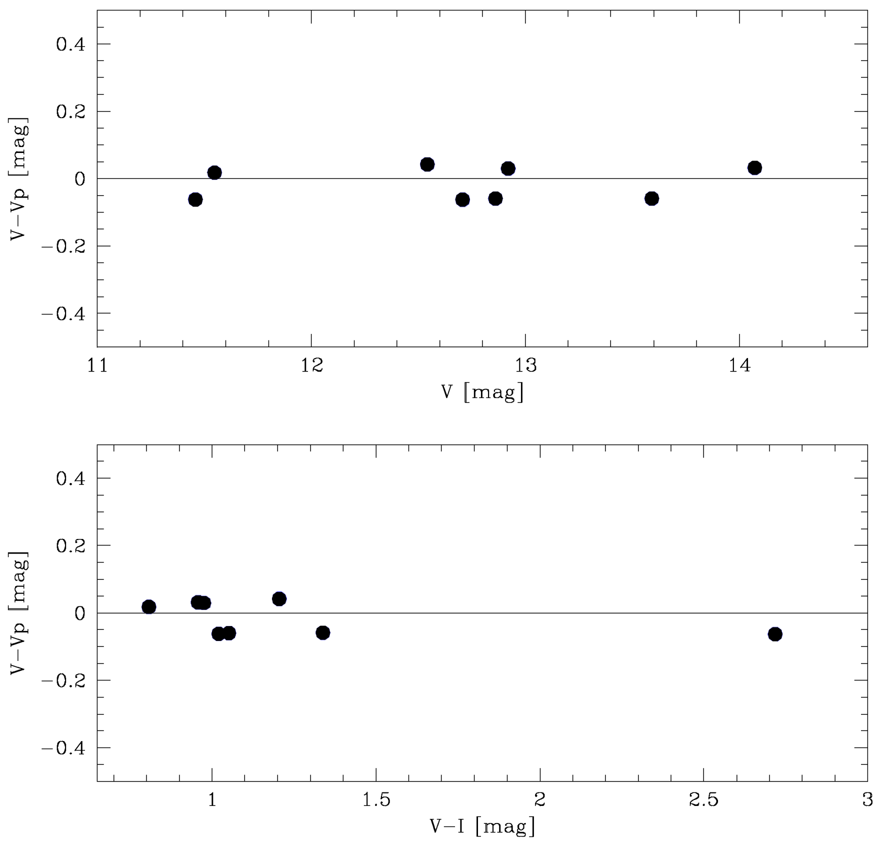

Fig. 1. The differences between *V*-band magnitudes calculated in this paper and taken from Hoag *et al.* (1961) for eight stars common to both studies, as a function of magnitude and color. A good agreement between both photometric zero points is demonstrated.

In order to convert our profile photometry to the aperture system, aperture corrections were derived in a very similar way as in Pietrzyński, Gieren and Udalski (2002). The final aperture correction was adopted as a median of aperture corrections derived for about 15 bright and well-isolated stars. The following values of the aperture corrections were obtained:

$$\mathrm{apc}(i) = -0.027 \pm 0.003, \qquad \mathrm{apc}(v) = -0.003 \pm 0.004.$$

To transform our instrumental magnitudes to the standard system of Landolt the following transformations very carefully established by Udalski (*et al.* 1998) were adopted:

$$V - I = 0.971 \cdot (v - i) + 0.362 \tag{1}$$
$$V = v + 0.006 \cdot (V - I) - 3.935 \tag{2}$$
$$I = i + 0.030 \cdot (V - I) - 4.367 \tag{3}$$

where the lowercase letters v and i denote the aperture instrumental magnitudes normalized to one second. The accuracy of the adopted zero points should be better than 0.04 mag in both bands.

In order to make an external check on the zero points of our photometry, we compared it with the results found in the literature. Unfortunately, because of the lack of data, we could compare our measurements with V-band photoelectric photometry only (Hoag *et al.* 1961). The mean difference is 0.015 ± 0.046 mag (see Fig. 1), so the both photometric zero points are consistent within the quoted uncertainties.

Having just one V-band measurement, we had to assume that the $V-I$ color was constant when transforming the light curves of the discovered variable stars to the standard system. Some very red stars were not detected on our V-band images, so in order to transform their light curves, we used the color of the reddest stars in clusters (*e.g.*, $V-I \approx 7.0$ mag). Please note that thanks to the fact that the color coefficients in Eqs. (2) and (3) are very small, these assumptions should not introduce significant errors on our calibrated magnitudes (in the worst cases they should not exceeded 0.003 mag in the V-band and 0.015 mag in the I-band).

The pixel (x,y) coordinates were transformed to the equatorial system based on the Digital Sky Survey (DSS) images using the procedure developed and used in the OGLE project (Udalski *et al.* 1998). The internal accuracy of obtained transformations should be better than $0\farcs3$.

5. Results

5.1. Photometric Data

The photometric and astrometric measurements for 16 595 stars in the field of NGC 6755 are presented in Table 2. The following data are provided: star number, equatorial coordinates, V and I-band magnitudes together with their corresponding errors returned by the DAOPHOT and $V-I$ color. Please note that the photometry of all stars brighter than about 12 mag in the I and 12.5 mag in the V-band is affected by the saturation problem. In the printed version of Table 2, we only give a subsample (10 first lines) of the data. The entire table can be obtained in the electronic form from the Acta Astronomica Archive (see cover page for details).

5.2. Detected Variable Stars

NGC 6755 is located in a dense region not very far from the Galactic Center. Therefore, strong contamination by the field stars and large and potentially variable extinction make the classification of the discovered variable stars and discussion on their cluster membership difficult.

In total seventy one new variable stars were discovered in the field of NGC 6755. Locations of all of them but some very red stars, which were not present on our V-band image, on the color-magnitude diagram (CMD) are shown in Fig. 2.

Table 2

Positions and photometry of stars in the field of NGC 6755

Id	α_{2000}	δ_{2000}	V [mag]	σ_V [mag]	I [mag]	σ_I [mag]	$V-I$ [mag]
1	$19^{h}07^{m}27^{s}.20$	$4^\circ09'50''.9$	10.281	0.025	6.770	0.037	3.599
4	$19^{h}07^{m}55^{s}.11$	$4^\circ11'50''.6$	11.617	0.025	9.177	0.011	2.535
5	$19^{h}07^{m}38^{s}.71$	$4^\circ13'02''.8$	11.812	0.013	9.312	0.011	2.595
6	$19^{h}07^{m}36^{s}.96$	$4^\circ13'37''.3$	10.356	0.022	9.464	0.008	0.995
7	$19^{h}07^{m}51^{s}.14$	$4^\circ10'35''.2$	11.418	0.016	9.761	0.014	1.756
8	$19^{h}07^{m}18^{s}.59$	$4^\circ10'38''.5$	12.165	0.012	9.812	0.009	2.448
9	$19^{h}07^{m}26^{s}.74$	$4^\circ13'37''.6$	11.758	0.064	9.859	0.011	1.996
9	$19^{h}07^{m}26^{s}.74$	$4^\circ13'37''.6$	12.942	0.185	9.893	0.011	3.139
10	$19^{h}07^{m}54^{s}.45$	$4^\circ13'54''.0$	12.179	0.011	9.902	0.040	2.374
11	$19^{h}07^{m}47^{s}.11$	$4^\circ20'17''.6$	12.707	0.010	10.083	0.011	2.717

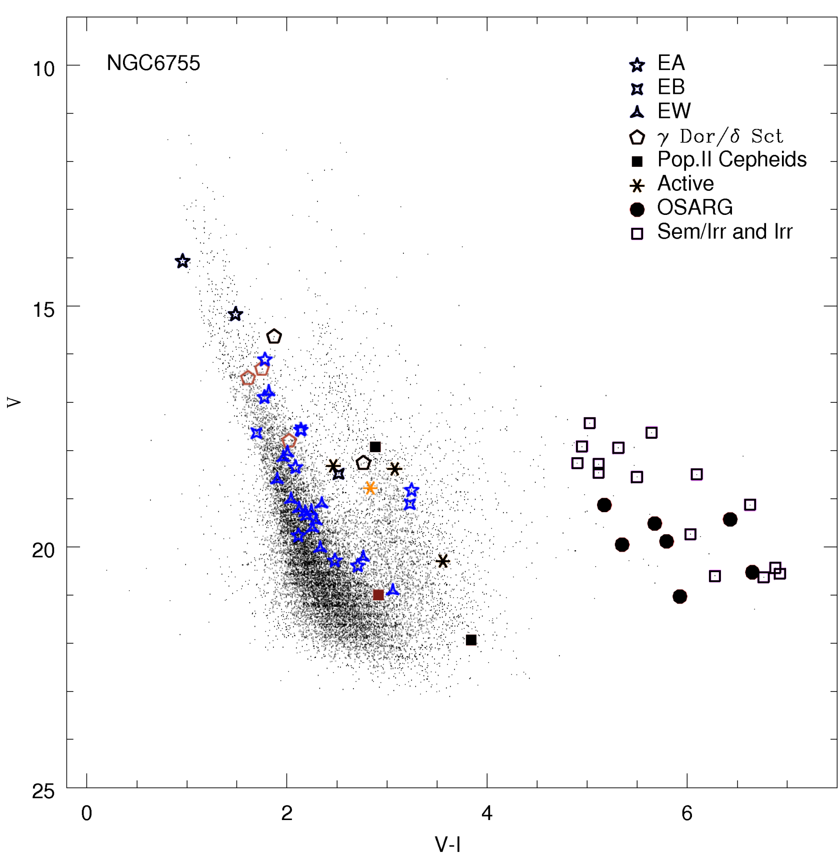

Fig. 2. Color–magnitude diagram for the open cluster NGC 6755. The position of different kinds of variable stars are marked with different symbols.

Please note that all the I-band magnitudes given in the tables below (*e.g.*, in Tables 3–6) are mean values computed from all observations collected in this filter for a given star, while the V-band magnitudes and $V-I$ colors are derived from the observations taken at HJD = 2451078.53

Eclipsing Binaries

Thirty one detected variable stars were classified as eclipsing binaries. Table 3 contains the temporary designation, equatorial coordinates, I and V-band magnitudes with corresponding errors, $V-I$ color, periods and times of brightness minima, when possible, for all of them. A sample of their light curves is presented in Fig. 3 and 4, while the positions on the CMD diagram are shown in Fig. 2.

Table 3

Eclipsing variable stars in NGC 6755

Name	α_{2000}	δ_{2000}	V [mag]	σ_V [mag]	I [mag]	σ_I [mag]	$V-I$ [mag]	P [days]	Phase	T_0 [HJD -2450000]	Type
V1	$19^h07^m59.^s14$	$4^\circ17'45.''9$	20.285	0.040	18.077	0.035	2.479	1.2026	0.8585	650.5765	EA
V2	$19^h07^m44.^s88$	$4^\circ10'32.''5$	18.823	0.017	15.674	0.010	3.246	24.3224	0.4524	1067.5311	EA
V3	$19^h07^m26.^s39$	$4^\circ15'12.''2$	16.893	0.009	15.221	0.009	1.775	–	–	–	EA
V4	$19^h07^m24.^s07$	$4^\circ12'26.''2$	16.111	0.010	14.464	0.010	1.781	–	–	–	EA
V5	$19^h07^m38.^s29$	$4^\circ18'22.''5$	20.393	0.055	18.037	0.034	2.707	1.77?	–	–	EA
V6	$19^h07^m44.^s74$	$4^\circ17'34.''2$	15.172	0.010	13.817	0.009	1.486	–	–	–	EA
V7	$19^h08^m01.^s29$	$4^\circ13'23.''0$	19.765	0.028	17.495	0.030	2.115	1.14?	–	–	EA
V8	$19^h08^m07.^s75$	$4^\circ19'28.''6$	18.350	0.016	16.427	0.016	2.086	0.75?	–	–	EA
V9	$19^h07^m48.^s19$	$4^\circ20'08.''8$	14.072	0.009	13.185	0.006	0.957	0.971?	–	–	EA
V10.2	$19^h07^m19.^s75$	$4^\circ15'39.''0$	17.575	0.011	14.921	0.013	2.140	1.1920	0.3039	646.6692	EA
V10.1			17.575	0.011	14.937	0.013	2.140	0.6743	0.6124	6735606	EB
V11	$19^h07^m40.^s76$	$4^\circ11'57.''8$	19.115	0.019	15.915	0.014	3.228	24.2911	0.4966	653.5233	EB
V12	$19^h08^m10.^s14$	$4^\circ13'26.''4$	18.486	0.016	16.066	0.019	2.517	4.1549	0.6291	664.5824	EB
V13	$19^h08^m03.^s62$	$4^\circ11'30.''3$	17.641	0.008	15.946	0.012	1.696	0.5989	0.9784	658.7265	EB
V14	$19^h07^m46.^s10$	$4^\circ09'54.''7$	18.150	0.035	16.346	0.019	1.964	0.7071	0.3056	674.5882	EW
V15	$19^h07^m50.^s76$	$4^\circ15'11.''5$	19.370	0.024	17.365	0.026	2.200	0.5443	0.6486	647.6095	EW
V16	$19^h07^m48.^s58$	$4^\circ18'20.''4$	19.285	0.031	17.341	0.033	2.184	0.7118	0.6874	668.7497	EW
V17	$19^h07^m59.^s14$	$4^\circ16'46.''0$	18.047	0.009	16.238	0.013	2.005	1.0639	0.1110	664.5525	EW
V18	$19^h08^m11.^s29$	$4^\circ16'34.''4$	16.785	0.009	15.037	0.017	1.818	0.8095	0.4120	647.5419	EW
V19	$19^h08^m04.^s44$	$4^\circ16'12.''2$	19.211	0.019	17.262	0.028	2.122	0.5048	0.1827	674.6353	EW
V20	$19^h07^m46.^s65$	$4^\circ19'41.''4$	19.615	0.037	17.488	0.032	2.257	0.4328	0.8116	649.7320	EW
V21	$19^h07^m28.^s66$	$4^\circ11'06.''9$	18.607	0.023	16.797	0.026	1.902	0.3779	0.230	674.5056	EW
V22	$19^h07^m21.^s89$	$4^\circ16'13.''5$	20.916	0.059	17.980	0.043	3.058	0.6486	0.6779	650.6618	EW
V23	$19^h08^m00.^s67$	$4^\circ10'19.''3$	19.020	0.016	17.112	0.018	2.041	0.3920	0.2706	647.6764	EW
V24	$19^h07^m52.^s17$	$4^\circ10'16.''3$	20.218	0.043	17.521	0.026	2.763	0.8196	0.1822	649.7562	EW
V25	$19^h08^m10.^s82$	$4^\circ10'20.''3$	20.027	0.037	17.762	0.029	2.334	0.4332	0.8013	649.7239	EW
V26	$19^h07^m30.^s22$	$4^\circ20'46.''8$	19.463	0.023	17.319	0.029	2.292	0.4990	0.3034	674.6688	EW
V27	$19^h07^m20.^s76$	$4^\circ20'47.''0$	19.110	0.028	16.768	0.032	2.347	0.7515	0.0071	654.7124	EW
V28	$19^h07^m53.^s64$	$4^\circ19'01.''7$	19.266	0.019	17.167	0.021	2.245	0.7708	0.1005	647.5920	EW
V29	$19^h07^m39.^s72$	$4^\circ12'40.''1$	–	–	18.330	0.043	–	0.3985	0.5255	654.7205	EW
V30	$19^h08^m14.^s39$	$4^\circ14'52.''1$	–	–	17.760	0.181	–	0.3556	–	647.7474	EW

Ten of discovered eclipsing binaries have light curves typical for EA-type systems. As can be seen in Fig. 2, the positions on the CMD diagram of all of them, except V2, are consistent with their cluster membership. The star designated as V2 is too red to belong to this young cluster, so most probably it is a background object. Unfortunately, our data were too scarce to derive any periods for V3, V4 and V6, whereas periods obtained for V5, V7, V8 and V9 should be treated as very preliminary.

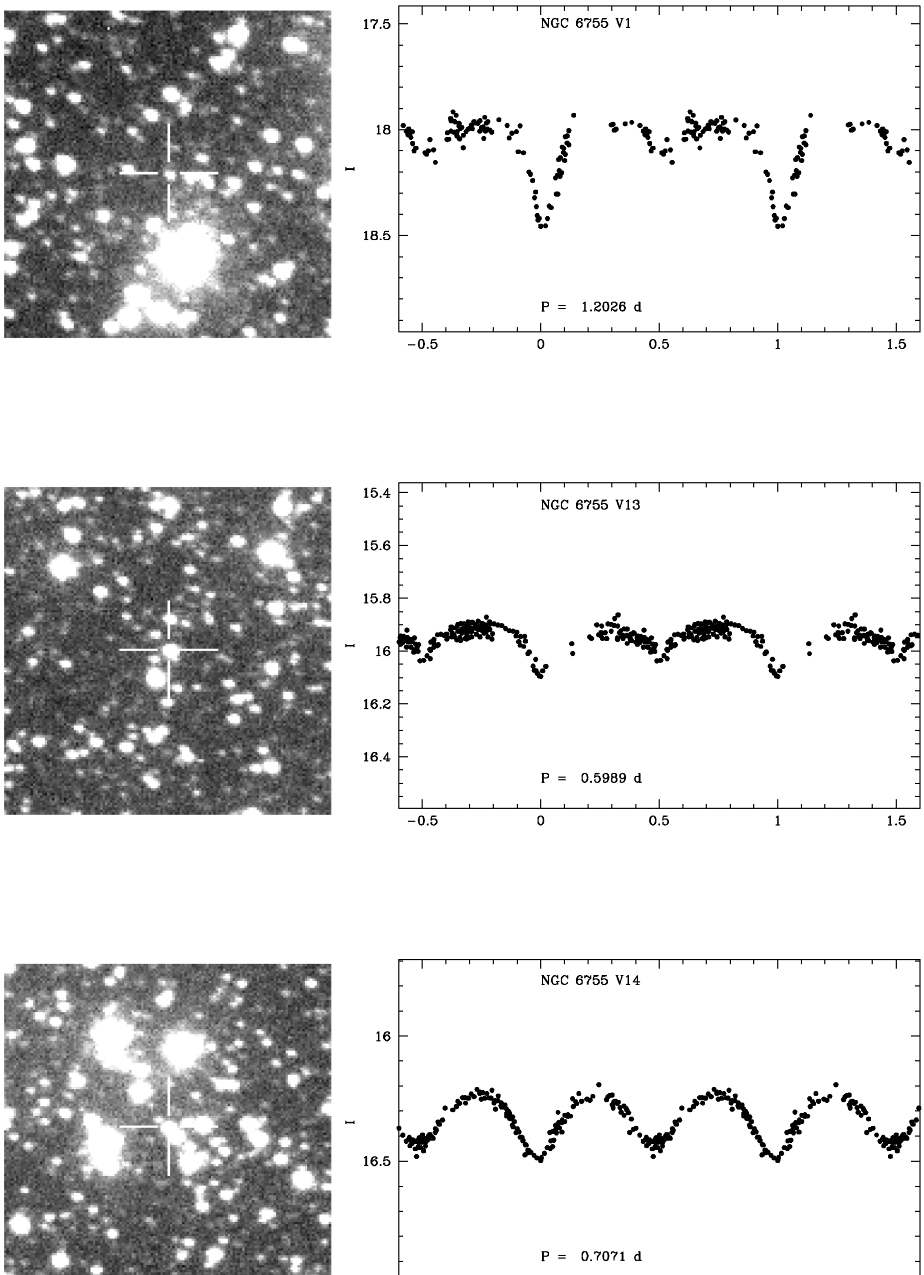

Fig. 3. Phased I-band light curves and finding charts of a sample of the detected eclipsing variable stars. The cross points the star. The size of the subframe is 1.5×1.5 arcmin. North is up, East to the left.

Next four objects (V10.1, V11, V12, V13), on account of the shape of their light curves, were classified as EB type eclipsing binary stars. The positions on the CMD diagram of two of them (V10.1 and V13) are consistent with their cluster membership. The remaining two objects have $V-I$ colors significantly redder than the main sequence stars, which are supposed to belong to the cluster, and therefore most probably are located behind the cluster.

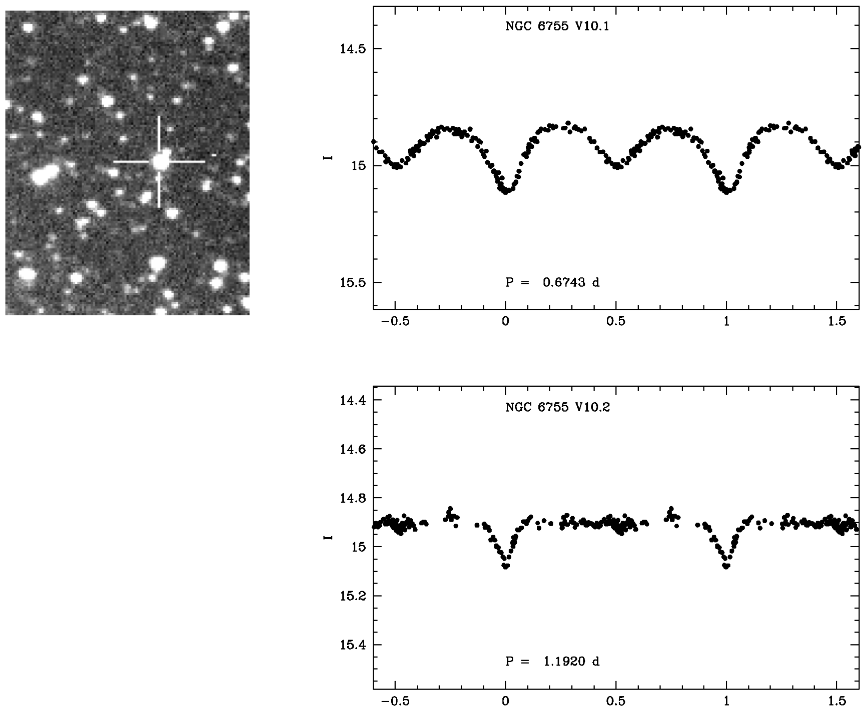

Fig. 4. Same as in Fig. 1, but for eclipsing systems V10.1 and V10.2 found within the same PSF.

Another seventeen of variable stars detected in the field of this cluster turned out to be EW-type eclipsing binaries. These stars are certainly too old to belong to this relatively young cluster. Probably they are placed closer than the cluster itself, so they are less reddened and on color–magnitude diagram have positions near the cluster main sequence.

The case of two binary stars V10.1 and V10.2 deserves a special attention since both of them were found within the same PSF (see Fig. 4). When we phased the light curve with the most prominent frequency found in the AoV periodogram, which corresponds to the period of 0.6124 days, we noticed a very large scatter, which indicated another kind of variability. After extraction of the light curve of the EB system with the period of 0.6124 days, we searched once again for possible periodicities. A clear peak in the AoV periodogram was identified at the period of 1.1920 days. As can be seen in Fig. 4, the light curve phased with this new period is typical for EA eclipsing systems. Most probably both stars are located within one PSF because of blending, but a physical connection of this object is not excluded.

Chromospherically Active Stars

The positions on the CMD of four of the detected variable stars suggest that they are anti centric late type stars. Table 4 contains information on temporary designation, equatorial coordinates, the I and V-band magnitude with errors, $V-I$ color and period of these stars. Their light curves are presented in Fig. 5. The small amplitude of the brightness variations are typical for late type, chromospherically active stars, so very tentatively we propose to include them into this group of variable stars.

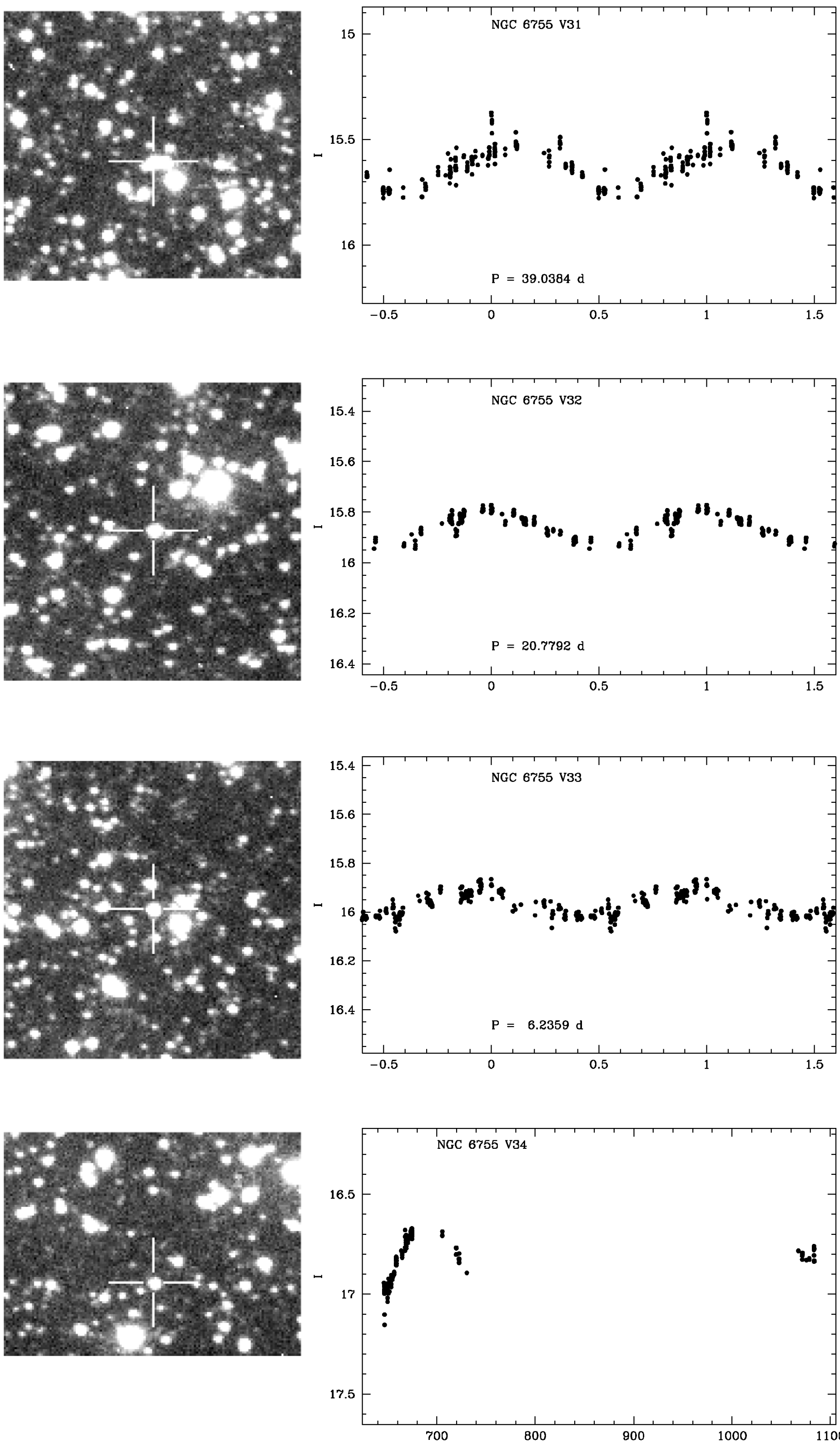

Fig. 5. *I*-band light curves of candidates for chromospherically active star: phased for V31, V32, V33 and non-phased for V34. The cross points the star. The size of the subframe is 1.5×1.5 arcmin. North is up, East to the left.

Table 4

Chromospherically active stars in NGC 6755

Name	α_{2000}	δ_{2000}	V [mag]	σ_V [mag]	I [mag]	σ_I [mag]	$V-I$ [mag]	P
V31	$19^{h}08^{m}12^{s}.35$	$4^\circ08'19''.5$	18.378	0.022	15.629	0.019	3.077	$39^{d}.0$
V32	$19^{h}07^{m}31^{s}.94$	$4^\circ14'41''.4$	18.316	0.014	15.842	0.012	2.463	$20^{d}.8$
V33	$19^{h}08^{m}06^{s}.92$	$4^\circ08'53''.2$	18.777	0.017	15.968	0.014	2.834	$6^{d}.236$
V34	$19^{h}07^{m}24^{s}.35$	$4^\circ08'11''.1$	20.297	0.042	16.833	0.017	3.558	–

γ Dor and δ Sct Variables

The location on the CMD diagram (see Fig. 2) and the light curves of V35, V36, V37 and V38, presented in Figs. 6 and 7, suggest that these objects belong to the γ Dor group of pulsating stars (Arentoft *et al.* 2007). In the cases of V37 and V38 two different periods for each of them, were detected. Two of our γ Dor candidates (V35, V36) may be cluster members, while the V37 and V38 are background objects.

The relatively short period, small amplitude and nearly sinusoidal shape of the light curve of the star designated temporary as V39, suggest that it is a δ Sct-type variable. The position on the CMD diagram of this object, shown in Fig. 2, does not exclude its cluster membership.

Table 5

Pulsating variable stars in NGC 6755

Name	α_{2000}	δ_{2000}	V [mag]	σ_V [mag]	I [mag]	σ_I [mag]	$V-I$ [mag]	P	Type
V35	$19^{h}07^{d}27^{s}.91$	$4^\circ15'08''.9$	16.498	0.009	14.959	0.009	1.612	$0^{d}.6374$	γ Dor
V36	$19^{h}08^{m}00^{s}.27$	$4^\circ08'47''.8$	16.304	0.009	14.679	0.009	1.751	$0^{d}.4950$	γ Dor
V37	$19^{h}07^{m}41^{s}.09$	$4^\circ15'54''.8$	17.801	0.015	15.819	0.018	2.023	$4^{d}.352$	γ Dor
								$0^{d}.8381$	
V38	$19^{h}07^{m}28^{s}.76$	$4^\circ18'54''.2$	18.259	0.013	15.575	0.011	2.764	$0^{d}.2641$	γ Dor
								$0^{d}.3586$	
V39	$19^{h}08^{m}02^{s}.21$	$4^\circ09'01''.6$	15.633	0.010	13.829	0.015	1.871	$0^{d}.1542$	δ Sct
V40	$19^{h}07^{m}22^{s}.46$	$4^\circ14'43''.3$	17.925	0.014	15.218	0.012	2.884	$41^{d}.61$	PopII
V41	$19^{h}07^{m}47^{s}.26$	$4^\circ19'30''.7$	20.992	0.073	18.134	0.036	2.914	$3^{d}.61$	PopII
V42	$19^{h}07^{m}23^{s}.82$	$4^\circ19'07''.1$	21.936	0.175	18.278	0.043	3.842	$13^{d}.23$	PopII or ell

The basic information (temporary designation, equatorial coordinates, standard I and V-band magnitude with errors, $V-I$ color) for the candidates for γ Dor and δ Sct stars, can be found in Table 5, their light curves are shown in Figs. 6 and 7.

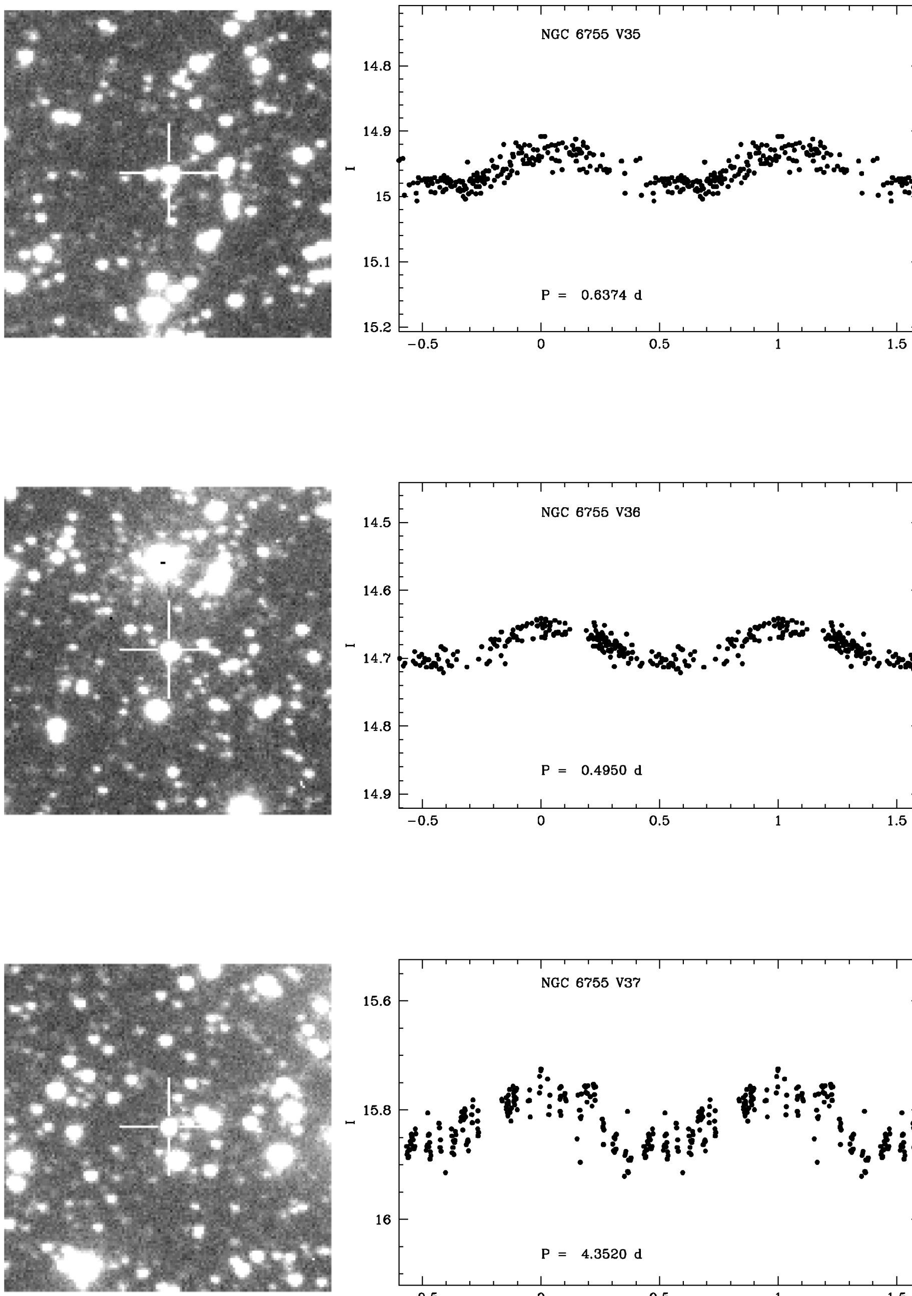

Fig. 6. Same as in Fig. 1, but for candidates for γ Dor-type variable stars: V35, V36 and V37 (primary period).

Population II Cepheids

The shape of the light curves of another three stars (V40, V41 and V42) resemble those of classical Cepheids (see Fig. 8). However, it would be very unlikely to detect three Cepheids in this direction on the sky and in a relatively small field of view we had. In order to verify the nature of these objects we adopted the typical colors of Cepheids with corresponding periods (Udalski *et al.* 1999b). Then, comparing them with the observed colors the reddenings were estimated. Finally,

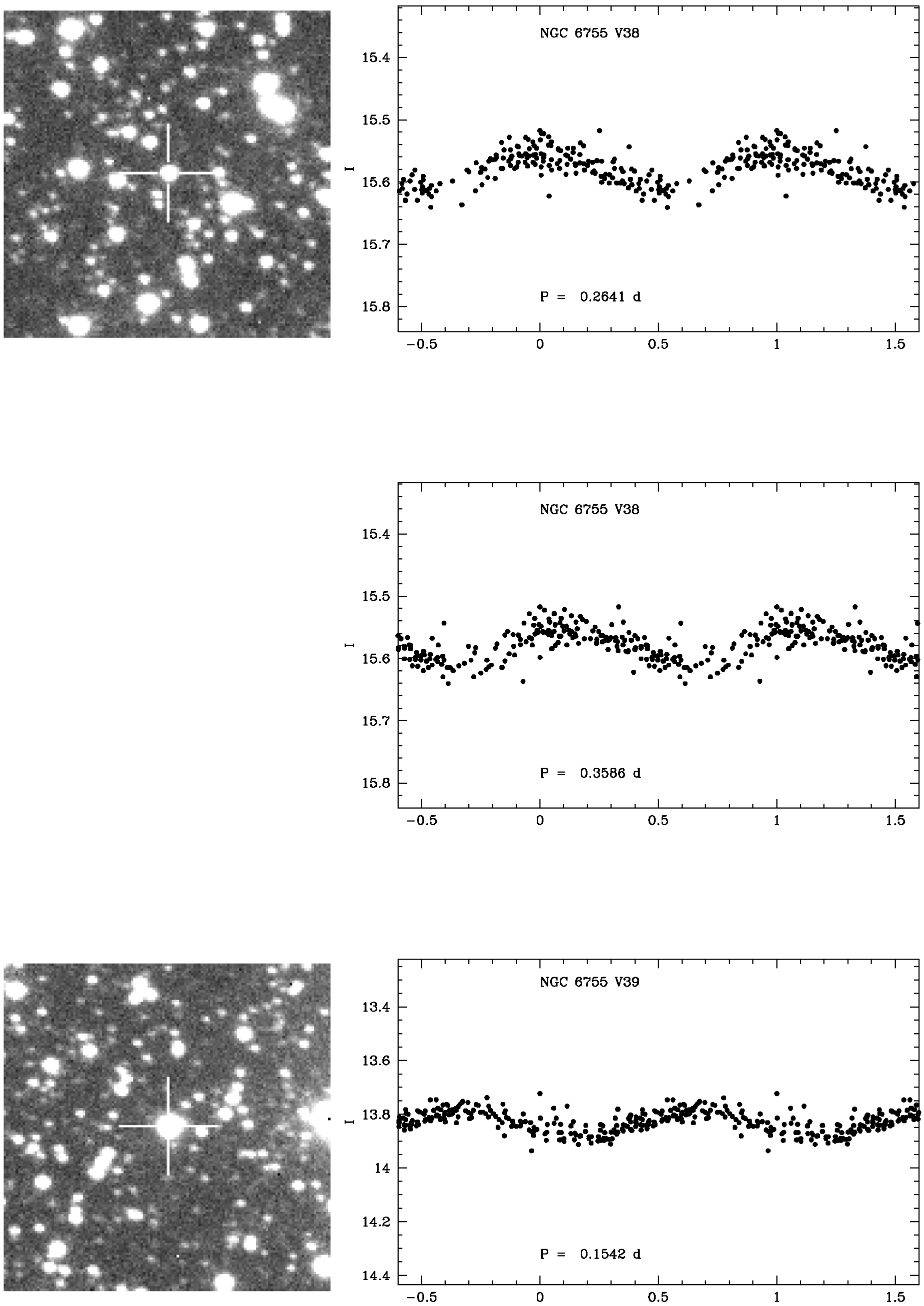

Fig. 7. Same as in Fig. 1, but for γ Dor-type candidate V38 (two possible periods) and δ Sct-type variable star V39.

assuming the Cepheid Period–Luminosity relation constructed by the OGLE group for the LMC Cepheids (Udalski *et al.* 1999a) we derived their approximate distances, which turned to be in the range from 17.0 mag to 17.8 mag. Therefore these stars could be anti centric population II Cepheids, which are about 2 mag fainter compared to classical Cepheids of the same period (see Kubiak and Udalski 2003, Wallerstein 2002). According to Wallerstein (2002) stars V41 and V42 should be classified as BL Her and W Vir, respectively. The case of the variable star desig-

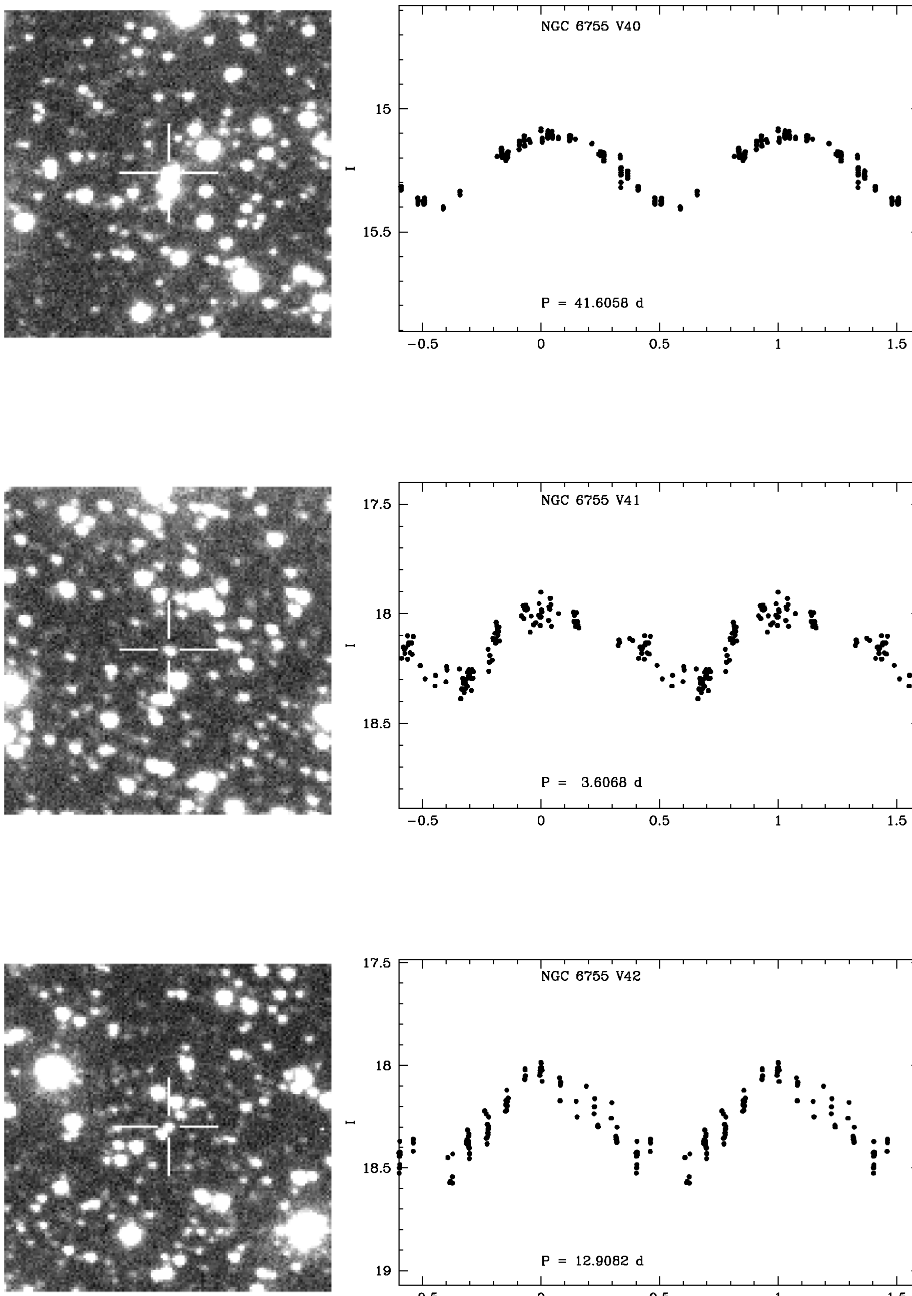

Fig. 8. Same as in Fig. 1, but for variable stars V40, V41 and V42. Stars V41 and V42 are most probably BL Her and W Vir variable stars, while V40 is either W Vir star with exceptionally long period or an ellipsoidal binary system with the period of about 82 days.

nated as V40 is not clear. Its period of about 41 days is longer than the conventional, but poorly established period limit of 20 days for W Vir stars (Wallerstein 2002). Nearly sinusoidal shape of the light curve and relatively small amplitude of this star does not exclude the possibility that this object is a binary system with a period of about 82 days. Therefore we conclude that the star V40 is either a W Vir star with an exceptionally long period or an ellipsoidal binary system with a strong reflexion effect. Equatorial coordinates, standard I and V-band magnitudes with formal DAOPHOT errors and $V-I$ colors of V40, V41 and V42 are given in Table 5.

Variable Red Giants

Next twenty eight of the detected variable stars are most probably highly obscured red giants from the background. Brightness of seven of them (V43, V44, V45, V46, V47, V48, V49) changes in the way typical for OGLE Small Amplitude Red Giant Stars (OSARGs; *e.g.*, Soszyński *et al.* 2004). Their very red colors and the fact that such stars are very common support this hypothesis. In the case of V45 the period two times longer is also possible. Light curves of a sample of these stars are presented in Fig. 9.

Table 6

Variable red giants in NGC 6755

Name	α_{2000}	δ_{2000}	V [mag]	σ_V [mag]	I [mag]	σ_I [mag]	$V-I$ [mag]	Type
V43	$19^h07^m57\overset{s}{.}82$	$4°10'43\overset{''}{.}5$	19.429	0.025	13.120	0.009	6.428	OSARG, $P\approx 30^d$
V44	$19^h07^m49\overset{s}{.}04$	$4°12'52\overset{''}{.}8$	19.954	0.036	14.726	0.009	5.351	OSARG, $P\approx 37\overset{d}{.}8$
V45	$19^h07^m32\overset{s}{.}33$	$4°19'05\overset{''}{.}2$	19.885	0.032	14.131	0.010	5.796	OSARG, $P\approx 28^d$
V46	$19^h07^m43\overset{s}{.}80$	$4°19'03\overset{''}{.}4$	19.512	0.023	13.986	0.008	5.677	OSARG, $P\approx 32\overset{d}{.}4$
V47	$19^h07^m37\overset{s}{.}13$	$4°20'02''$	21.028	0.089	15.178	0.009	5.929	OSARG, $P\approx 56^d$
V48	$19^h07^m47\overset{s}{.}42$	$4°19'58\overset{''}{.}2$	19.132	0.018	13.978	0.006	5.173	OSARG, $P\approx 23^d$???
V49	$19^h07^m53\overset{s}{.}54$	$4°17'49\overset{''}{.}1$	20.525	0.090	13.869	0.008	6.652	OSARG, $P\approx 74\overset{d}{.}8$
V50	$19^h07^m21\overset{s}{.}12$	$4°11'30\overset{''}{.}9$	18.283	0.015	13.318	0.007	5.116	Irr/sem
V51	$19^h07^m44\overset{s}{.}79$	$4°08'10\overset{''}{.}8$	20.559	0.049	13.810	0.009	6.926	Irr/sem
V52	$19^h07^m41\overset{s}{.}77$	$4°11'48\overset{''}{.}9$	20.602	0.056	14.475	0.009	6.279	Irr/sem
V53	$19^h08^m00\overset{s}{.}37$	$4°09'02\overset{''}{.}9$	18.497	0.015	12.558	0.008	6.095	Irr/sem
V54	$19^h07^m59\overset{s}{.}64$	$4°09'22\overset{''}{.}3$	19.128	0.019	12.678	0.010	6.629	Irr/sem
V55	$19^h07^m46\overset{s}{.}09$	$4°16'36\overset{''}{.}1$	18.261	0.014	13.417	0.006	4.903	Irr/sem
V56	$19^h07^m37\overset{s}{.}49$	$4°18'26\overset{''}{.}0$	18.460	0.014	13.558	0.006	5.116	Irr/sem
V57	$19^h07^m53\overset{s}{.}72$	$4°18'51\overset{''}{.}3$	–	–	13.705	0.021	–	Irr/sem
V58	$19^h07^m21\overset{s}{.}51$	$4°21'20\overset{''}{.}2$	–	–	15.532	0.011	–	Irr/sem
V59	$19^h07^m20\overset{s}{.}54$	$4°21'30\overset{''}{.}6$	–	–	14.584	0.177	–	Irr/sem
V60	$19^h08^m13\overset{s}{.}16$	$4°21'54\overset{''}{.}5$	–	–	15.890	0.177	–	Irr/sem
V61	$19^h08^m05\overset{s}{.}71$	$4°12'06\overset{''}{.}7$	17.920	0.010	13.113	0.008	4.948	Irregular
V62	$19^h07^m42\overset{s}{.}90$	$4°14'32\overset{''}{.}4$	18.551	0.013	13.131	0.008	5.499	Irregular
V63	$19^h07^m39\overset{s}{.}64$	$4°14'55\overset{''}{.}5$	20.436	0.041	13.750	0.009	6.882	Irregular
V64	$19^h07^m33\overset{s}{.}87$	$4°14'07\overset{''}{.}4$	19.737	0.028	13.722	0.008	6.034	Irregular
V65	$19^h08^m06\overset{s}{.}87$	$4°13'16\overset{''}{.}7$	17.430	0.008	12.541	0.009	5.029	Irregular
V66	$19^h07^m22\overset{s}{.}26$	$4°18'49\overset{''}{.}3$	17.945	0.011	12.749	0.010	5.313	Irregular
V67	$19^h07^m22\overset{s}{.}31$	$4°15'10\overset{''}{.}9$	20.629	0.057	13.953	0.011	6.765	Irregular
V68	$19^h07^m47\overset{s}{.}20$	$4°18'18\overset{''}{.}6$	17.628	0.014	11.961	0.007	5.647	Irregular
V69	$19^h08^m12\overset{s}{.}62$	$4°18'57\overset{''}{.}2$	–	–	14.985	0.009	–	Irregular
V70	$19^h07^m34\overset{s}{.}47$	$4°21'34\overset{''}{.}5$	–	–	12.711	0.177	–	Irregular

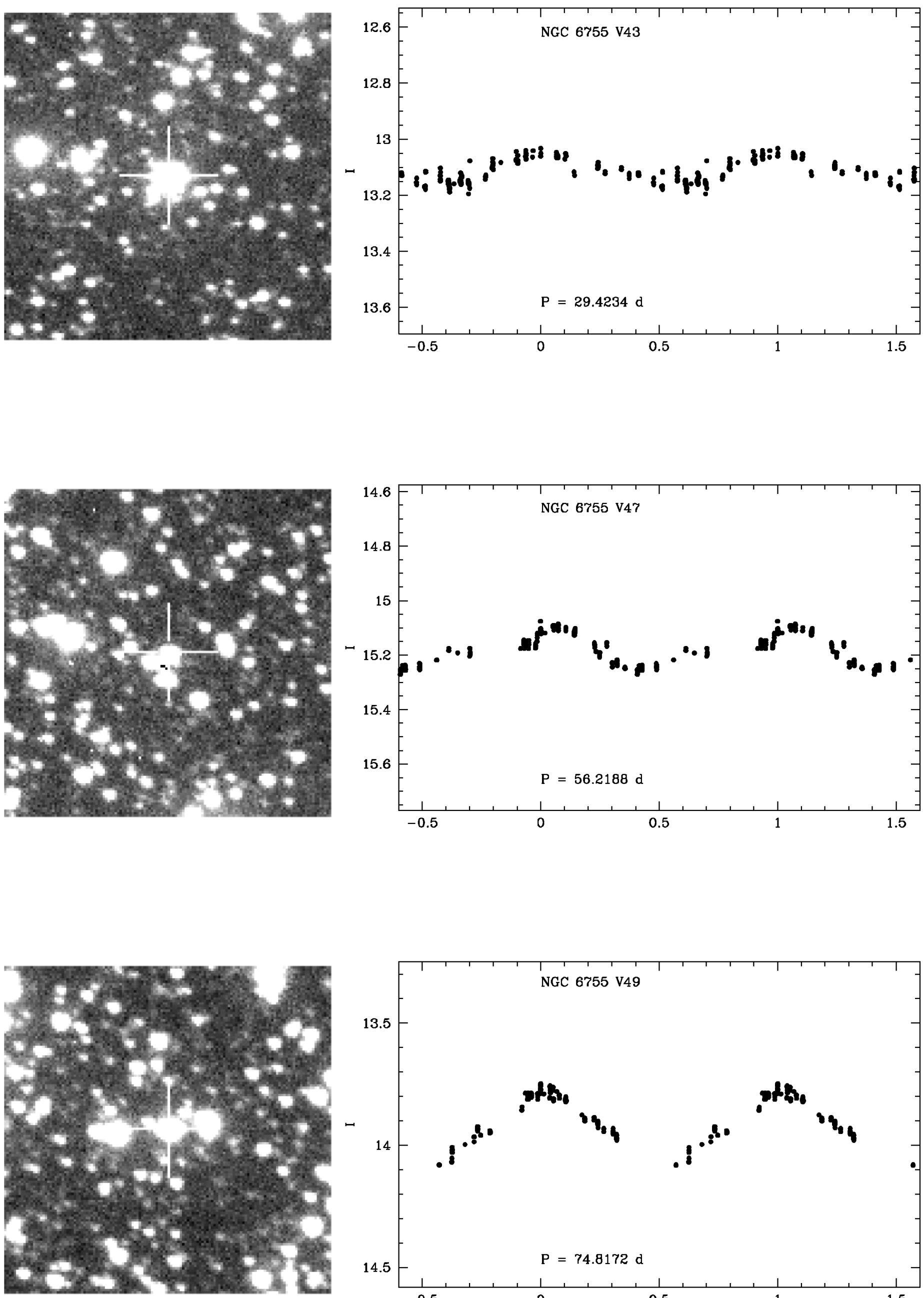

Fig. 9. Same as in Fig. 1, but for OSARG type variable stars: V43, V47 and V49.

The remaining twenty one variable stars due to their photometric behavior and positions on the CMD are temporarily classified as irregular red giants. It is very probable that with the additional photometric data covering larger time baseline some of them could turn out to be OSARGs or other type of variable red giant stars as well. Three exemplary light curves of this group are displayed in Fig. 10. Basic information (temporary designation, equatorial coordinates, the I and V-band magnitude with errors, $V-I$ color) on all stars discussed in this Section is given in Table 6.

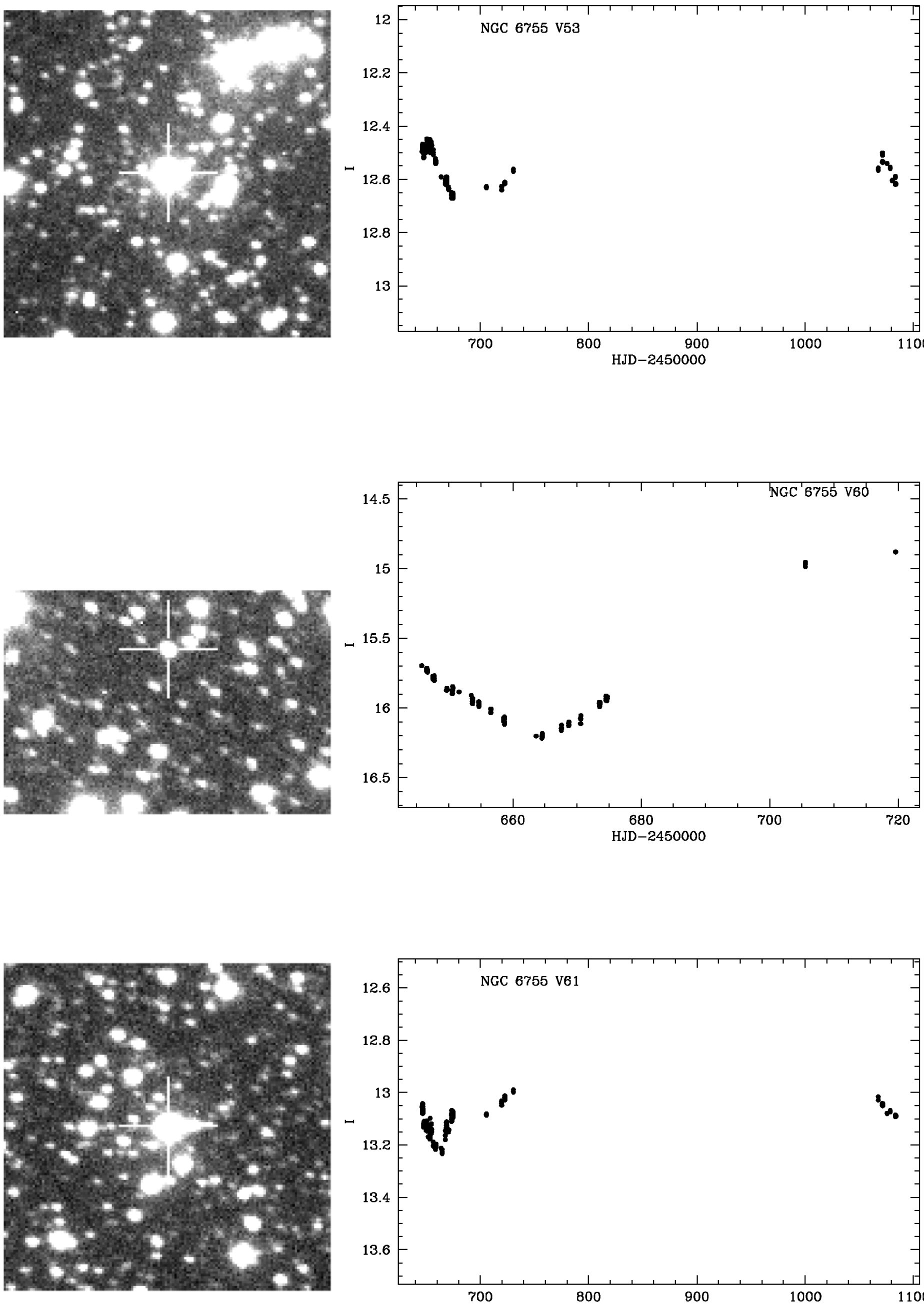

Fig. 10. *I*-band light curves and finding charts for irregular variable stars: V53, V60 and V61. The cross points the star. The size of the subframe is 1.5×1.5 arcmin. North is up, East to the left.

6. Summary

A deep CCD photometry (down to 23 mag in *V*) and astrometry for some 16 600 stars located in the $14' \times 14'$ region centered on the open cluster NGC 6755 are presented. Based on 173 *I*-band images collected over a period of two years seventy one variable stars were identified. Thirty one of them were reckoned as eclipsing binaries. Seventeen EW-type stars are too old to belong to this relatively young open cluster. The cluster membership of one EA and two EB systems can also be excluded based on their position on the CMD diagram, while the location on the CMD diagram of the remaining nine EA and two EB binaries is consistent with their cluster membership. Next five of the discovered variables are located in the expected main instability strip. Four of them we classified as γ Dor, and one as δ Sct star. Two γ Dor stars and the δ Sct star may belong to the cluster. Another three stars were assumed to be anti centric Cepheids of Population II, while V40 could also be an ellipsoidal binary system. Twenty eight of the discovered variable stars are most probably highly obscured red giants. Seven of them revealed photometric variability typical for OSARGs, whereas the remaining twenty one red giants showed irregular changes of their brightness.

All photometric measurements and finding charts for detected variable stars can be download from the Acta Astronomica Archive.

Additional photometric data would be very useful to establish periods for several eclipsing binaries, while the spectroscopic observations are needed to verify membership of the detected variable stars.

Acknowledgements. This research has made use of the WEBDA database, operated at the Institute for Astronomy of the University of Vienna. The paper was supported by the MNiSW BST and BW grants to Warsaw University Observatory.

REFERENCES

Arentoft, T., *et al.* 2007, *Astron. Astrophys.*, **465**, 965.
Ciechanowska, A., Pietrzyński, G., Wyrzykowski, Ł., Szewczyk, O., Kubiak, M., Udalski, A., and Szymański, M.K. 2006, *Acta Astron.*, **56**, 219.
Hoag, A., Johnson, H., Iriarte, B., Mitchell, R., Hallam, K., and Sharpless, S. 1961, *PUSNO*, **17**, 347.
Kubiak, M., and Udalski, A. 2003, *Acta Astron.*, **53**, 117.
Kjeldsen, H., and Frandsen, S. 1991, *Astron. Astrophys. Suppl. Ser.*, **87**, 119.
Pietrzyński, G. 1996a, *Acta Astron.*, **46**, 287.
Pietrzyński, G. 1996b, *Acta Astron.*, **46**, 349.
Pietrzyński, G. 1997, *Acta Astron.*, **47**, 211.
Pietrzyński, G., Kubiak, M., Udalski, A., and Szymański, M. 1997, *Acta Astron.*, **47**, 437.
Pietrzyński, G., Kubiak, M., Udalski, A., and Szymański, M. 1998, *Acta Astron.*, **48**, 489.
Pietrzyński, G., Wyrzykowski, Ł., Szewczyk, O., and Bielewicz, M. 2001, *Acta Astron.*, **51**, 65.
Pietrzyński, G., Gieren, W., and Udalski, A. 2002, *P.A.S.P.*, **114**, 298.
Schwarzenberg-Czerny, A. 1989, *MNRAS*, **241**, 153.
Soszyński, I., *et al.* 2004, *Acta Astron.*, **54**, 347.
Udalski, A., Kubiak, M., and Szymański, M. 1997, *Acta Astron.*, **47**, 319.
Udalski, A., Szymański, M., Kubiak, M., Pietrzyński, G., Woźniak, P., and Żebruń, K. 1998, *Acta Astron.*, **48**, 147.
Udalski, A., Szymański, M., Kubiak, M., Pietrzyński, G., Soszyński, I., Woźniak, P., and Żebruń, K. 1999a, *Acta Astron.*, **49**, 201.
Udalski, A., Soszyński, I., Szymański, M., Kubiak, M., Pietrzyński, G., Woźniak, P., and Żebruń, K. 1999b, *Acta Astron.*, **49**, 223.
Wallerstein, G. 2002, *P.A.S.P.*, **114**, 689.
Wyrzykowski, Ł., Pietrzyński, G., and Szewczyk,O. 2002, *Acta Astron.*, **52**, 105.